

RESEARCH

Open Access



Effects of *Bifidobacterium* and rosuvastatin on metabolic-associated fatty liver disease via the gut–liver axis

Xue Ran^{1†}, Ying-jie Wang^{2†}, Shi-gang Li^{3*†} and Chi-bing Dai^{1*†}

Abstract

Background/aims Research has indicated that treatment with *rosuvastatin* can improve liver pathology in metabolic-associated fatty liver disease (MAFLD) patients and that treatment with *Bifidobacterium* can improve MAFLD. Therefore, the effects of *Bifidobacterium*, *rosuvastatin*, and their combination on related indices in a rat model of diet-induced MAFLD need to be investigated.

Methods Forty rats were divided into five groups: the normal diet group (N), high-fat diet (HFD) model group (M), HFD + probiotic group (P), HFD + statin group (S), and HFD + probiotic + statin group (P-S). To establish the MAFLD model, the rats in Groups M, P, S, and P-S were fed a HFD for 8 weeks. The treatments included saline in Group N and either *Bifidobacterium*, *rosuvastatin*, or their combination in Groups P, S, and P-S by intragastrical gavage. After 4 weeks of intervention, the rats were euthanized, and samples were harvested to analyze gastrointestinal motility and liver function, pathological changes, inflammatory cytokine production, and the expression of proteins in key signaling pathways.

Results HFD feeding significantly increased the body weight, liver index, and insulin resistance (IR) index of the rats, indicating that the MAFLD model was successfully induced. *Bifidobacterium* reduced the liver of MAFLD rats, while *Bifidobacterium* with *Rosuvastatin* decreased the liver index, IR index, and levels of aspartate aminotransferase and alanine aminotransferase in MAFLD rats. The MAFLD model showed altered expression of proteins in signaling pathways that regulate inflammation, increased production of inflammatory cytokines, an elevated MAFLD activity score (MAS), and pathological changes in the liver. The MAFLD model also showed reduced relative counts of intestinal neurons and enteric glial cells (EGCs), altered secretion of gastrointestinal hormones, and slowed gastrointestinal emptying. *Bifidobacterium*, *rosuvastatin*, or their combination inhibited these various changes. HFD feeding changed the rats' gut microbiota, and the tested treatments inhibited these changes. These results suggest that the gastrointestinal motility disorder and abnormal liver function in MAFLD rats may be related to a reduction in *Escherichia-Shigella* bacteria and an increase in *Asticcacaulis* bacteria in the gut microbiota and that the improvement in liver function

[†]Xue Ran and Ying-jie Wang are co-first authors and contributed equally to this work.

[†]Shi-gang Li and Chi-bing Dai are co-corresponding authors and contributed equally to this study.

*Correspondence:

Shi-gang Li

fox201@163.com

Chi-bing Dai

dchibing@126.com

Full list of author information is available at the end of the article



© The Author(s) 2024. **Open Access** This article is licensed under a Creative Commons Attribution-NonCommercial-NoDerivatives 4.0 International License, which permits any non-commercial use, sharing, distribution and reproduction in any medium or format, as long as you give appropriate credit to the original author(s) and the source, provide a link to the Creative Commons licence, and indicate if you modified the licensed material. You do not have permission under this licence to share adapted material derived from this article or parts of it. The images or other third party material in this article are included in the article's Creative Commons licence, unless indicated otherwise in a credit line to the material. If material is not included in the article's Creative Commons licence and your intended use is not permitted by statutory regulation or exceeds the permitted use, you will need to obtain permission directly from the copyright holder. To view a copy of this licence, visit <http://creativecommons.org/licenses/by-nc-nd/4.0/>.

induced by *Bifidobacterium* plus *rosuvastatin* may be related to increases in *Sphingomonas* and *Odoribacter* bacteria and a decrease in *Turicibacter* bacteria in the gut microbiota.

Conclusions The combined use of *Bifidobacterium* and *rosuvastatin* could better regulate the gut microbiota of MAFLD model rats, promote gastrointestinal emptying, and improve liver pathology and function than single treatment with *Bifidobacterium* or *rosuvastatin*. This provides a better strategy for the treatment of MAFLD.

Keywords Metabolic-associated fatty liver disease, *Bifidobacterium*, *Rosuvastatin*, Gut microbiota, Gastrointestinal motility

Introduction

Metabolic-associated fatty liver disease (MAFLD) occurs when excessive fat accumulates in hepatocytes in conjunction with hepatocellular steatosis and is diagnosed only after the exclusion of other definitive factors known to cause liver damage [1, 2]. MAFLD is related to insulin resistance (IR) and genetic susceptibility [3]. As the most common chronic liver disease worldwide, MAFLD had a global prevalence of 29.8% according to an epidemiological study [4]. Metabolic-associated steatohepatitis (MASH), hepatocellular carcinoma (HCC), and cirrhosis are all forms of MAFLD that not only can lead to liver dysfunction and death [5] but are also high-risk factors for diseases such as cardiovascular disease [6], metabolic syndrome [7], type 2 diabetes [8], and chronic kidney disease [9]. In the United States, MASH represents the leading and second leading cause of liver transplantation in women and men, respectively [10]. Current pharmacological treatments for MAFLD include lipid-lowering agents, insulin sensitizers, cytoprotective agents, and antioxidants [2, 11], but these drugs have adverse effects on long-term use. Therefore, for better treatment of MAFLD, the development of effective and safe therapeutic agents is critically needed.

The “multiple hits” theory is the most widely accepted theory for explaining the complex pathogenesis of MAFLD. Both environmental and genetic factors, as well as neuroendocrine dysregulation, oxidative stress, the inflammatory response, dysbiosis of the gut microbiota, and other factors, together lead to the occurrence and progression of MAFLD [12, 13]. Gut microbiota dysbiosis is an important factor suggested to lead to MAFLD in the “multiple hits” theory. Because the gut and liver have the same embryonic origin and are connected via the hepatic portal system, the concept of the gut–liver axis was proposed [14]. In the human body, the gut microbiota and its metabolic products may participate in most physiological functions, including nutrient conversion, absorption and metabolism, vitamin synthesis, and immune regulation, via the gut–liver axis [15]. Moreover, the gut microbiota can also affect the occurrence and development of MAFLD by altering

intestinal permeability, interfering with lipid metabolism, and producing endogenous ethanol; accordingly, the gut microbiota is considered a potential therapeutic target for MAFLD [16, 17]. In the development of such therapies, the changes in the gut microbiota in MAFLD patients need to be fully characterized.

Bifidobacterium is a classical probiotic and an active microorganism that has health benefits for the host. Multiple studies [18, 19] have shown that *Bifidobacterium* can lower the IR index, reduce fat accumulation, lower serum inflammatory cytokine levels, and improve the symptoms and pathophysiology of MAFLD, but the exact mechanism remains unclear. Statins are used to treat hypercholesterolemia clinically, and recent research [20] has demonstrated that statins can prevent HCC associated with MAFLD and MASH, whereas *rosuvastatin* can improve the histological changes within the liver observed in MASH. In addition, it is unclear whether there is a difference in the efficacy of *Bifidobacterium* and *rosuvastatin* in MAFLD and whether the combined effect of the two is more obvious. Therefore, an in-depth study of the actions of *Bifidobacterium*, *rosuvastatin* and their combination in MAFLD, as well as the underlying mechanisms, was conducted, as the results are expected to have important theoretical and practical significance for the prevention and prognosis of MAFLD.

In the present study, a MAFLD rat model was established by feeding a high-fat diet (HFD), and the effects of treatment with *Bifidobacterium*, *rosuvastatin*, or their combination on body weight, energy intake, the liver index, IR index, liver function, blood lipid levels, the MAFLD activity score (MAS), gastrointestinal motility, enteric nervous system (ENS) function, the gut microbiota, gastrointestinal hormone levels, and the expression levels of proteins of the Toll-like receptor-4 (TLR-4)/nuclear factor kappa B (NF- κ B) and AMP-activated protein kinase (AMPK)/nuclear factor erythroid 2-related factor 2 (Nrf2) pathways were analyzed. This study aimed to further clarify the curative effects and mechanisms of *Bifidobacterium*, *rosuvastatin* and their combination in the treatment of MAFLD.

Materials and methods

Animals

Four-week-old male, specific pathogen-free Sprague–Dawley rats were purchased from and housed at the Three Gorges University Laboratory Animal Center (Yichang, Hubei Province, China) under a 12-h light/dark cycle under specific pathogen-free conditions, 50–70% relative humidity, and a temperature of 22 ± 2 °C. The physical activity and excrement of the rats were observed every day. The body weight of each rat and the food intake of each group of rats were measured weekly, and the energy intake of each rat was calculated via the following formula:

The energy intake of each rat in Group N = the food intake of each group $\times 1.08/n$ (n is the number of rats in each group).

The energy intake of each rat in Group M, S, P, P–S = the food intake of each group $\times 3.11/n$ (n is the number of rats in each group).

After being fed a normal diet for 1 week, 40 rats were randomly divided into five groups: Groups N, M, P, S and P–S ($n = 8$ each). Only Group N continued to receive a normal diet, whereas the other four groups were fed a HFD (Nanjing Shengmin Scientific Research Co., Ltd., Nanjing, China) for 8 weeks. The normal diet consisted of 0.82% lysine, 4% crude fat, 18% crude protein, and 0.53% methionine + cystine (1.08 kcal/g), whereas the HFD contained 20% lard, 16% sugar, 2% cholesterol, 0.2% bile salts, and 61.8% normal diet (3.11 kcal/g). Food and water intake were unrestricted for all the rats.

After 8 weeks, the rat with the greatest weight difference in each group was excluded, and then one remaining rat in each group was randomly sacrificed for harvesting of liver tissue, which was stained with hematoxylin and eosin (HE) for evaluation of the MAFLD activity score (MAS) [21] (Table 1) by two pathologists blinded to all groups. The MAFLD model was assumed to be established if the MAS was ≥ 3 . The rats were fed the same diet as before and given the following different interventions by gavage once daily for 4 weeks: 2 mL of saline for Groups N and M; 1×10^{10} colony-forming units (CFUs) of *Bifidobacterium* (Nuofan Biotechnology Co., Ltd., Wuhan, China) dissolved in 2 mL of saline for Group P; 1.08 mg/kg *rosuvastatin* calcium tablets (Zhejiang Hisun

Pharmaceutical Co., Ltd., Zhejiang, China) dissolved in 2 mL of saline for Group S; and 1×10^{10} CFU of *Bifidobacterium* + 1.08 mg/kg *rosuvastatin* calcium tablets dissolved in 2 mL of saline for Groups P–S.

The Animal Ethics Committee of China Three Gorges University approved all the experimental protocols involving rats, and the Institutional Animal Care and Use Committee of Three Gorges University approved all the treatment procedures (No: 2021ky90). During the 4 weeks of intervention, food intake and body weight were measured once per week for the rats in all the groups.

Tissue sample and fecal sample collection

After the intervention, all the rats were fasted overnight and then weighed. Two milliliters of a black nutritive semisolid paste [22] was given to these rats. Each 2 mL dose weighed 1.835 g and was delivered by intragastric administration. One hour later, the rats were anesthetized via an intraperitoneal injection of 10% chloral hydrate (0.3 mL/100 g). The abdominal cavity was then opened, and blood was collected from the abdominal aorta. The ligaments around the liver were separated for removal, and the liver was weighed after being cleaned with saline and sterile gauze. The two ends of the stomach were ligated, and then the stomach was removed, cleaned with saline and sterile gauze, and weighed to obtain the total weight of the stomach. Next, the stomach was cut, and the contents were rinsed out to obtain the net weight. The small intestine and large intestine were subsequently removed and placed on a sterile sheet in its natural state. The total length of the small intestine and the length of the small intestine portion that was stained black were measured. Finally, a sample of colon tissue 6–8 cm away from the anus was collected and fixed in 4% paraformaldehyde, and fecal samples were collected in sterile Eppendorf tubes. The liver index, gastric emptying rate, and intestinal propulsion rate were calculated via the following formulae:

Liver index = whole liver weight/total body weight $\times 100\%$

Table 1 Rubric for determining the MAFLD activity score (MAS)

Score	0	1	2	3
Hepatic steatosis	< 5%	5% ~ 33%	34% ~ 66%	66%
Inflammation in hepatic lobules	0	< 2	2 ~ 4	> 4
Ballooning degeneration of liver cells	none	less	more	-----

$$\text{Gastric emptying rate} = 1 - (\text{stomach total weight} - \text{stomach net weight}) / 1.835 \times 100\%$$

$$\text{Intestinal propulsion rate} = \text{length of small intestine stained black} / \text{total length of small intestine} \times 100\%$$

Liver pathology and serum index detection

Portions of liver tissues were soaked and fixed with 4% neutral formaldehyde, and following standard protocols, hematoxylin and eosin (HE) staining of the sections was performed.

Blood samples were centrifuged at 3000 rpm and 4 °C for 10 min (Centrifuge: C2500-R-230 V, Labnet, NJ, USA). The recovered supernatant samples were separated into 200-μL tubes, and enzyme-linked immunosorbent assay (ELISA) kits (Elabscience Biotechnology Co., Ltd., Wuhan, China) were used following the manufacturer's instructions to measure the concentrations of gastrin (GT), somatostatin (SST), vasoactive intestinal peptide (VIP), and 5-hydroxytryptamine (5-HT) in the serum. ELISA kits (Beijing Strong Biotechnologies, Inc., Beijing, China) were used to measure the concentrations of high-density lipoprotein (HDL), total cholesterol (TC), triglycerides (TG), low-density lipoprotein (LDL), insulin (INS), and fasting blood glucose (FBG). ELISA kits (Shanghai Fosun Long March Medical Science Co., Ltd., Shanghai, China) were used to measure the concentrations of aspartate aminotransferase (AST) and alanine aminotransferase (ALT). The insulin resistance index (IR index) was calculated as follows:

$$\text{IR index} = (\text{FBG} \times \text{INS}) / 22.5$$

Cytokine and protein expression in liver tissue

To prepare the liver tissue supernatant, a portion of liver tissue was weighed, and saline was subsequently added to prepare a homogenate with a weight (g)-to-volume (mL) ratio of 1:9 (Homogenate: TissueLyser-241, Shanghai Jingxin Industrial Development Co., Ltd., Shanghai, China). After the homogenate was centrifuged at 3500 rpm and 4 °C for 10 min (centrifuge: C2500-R-230 V, Labnet, NJ, USA), the supernatant was collected to detect the concentrations of interleukin 6 (IL-6), interleukin 1 beta (IL-1β), and tumor necrosis factor alpha (TNF-α) via ELISA kits (Elabscience Biotechnology Co., Ltd., Wuhan, China).

For detection of the expression of related proteins, samples of liver tissue were cut into pieces and placed in Eppendorf tubes. Cleaned steel beads were added, as were 200 μL of single decontaminant lysate, which contained 2 μL of phenylmethanesulfonyl fluoride (PMSF; Aladdin

Biochemical Technology Co., Ltd., Shanghai, China) and 2 μL of phosphatase inhibitor (Beyotime Biotechnology, Shanghai, China). The tubes were then placed in a TissueLyser-24 (Jingxin Technology Co., Ltd., Shanghai, China) and then on ice for 30 min to fully lyse the tissue samples. After the lysate was centrifuged, the supernatant was collected in fresh tubes. A BCA kit (Beyotime Biotechnology, Shanghai, China) was used to determine the total protein concentration. The protein lysates (40 μg/well) were separated on gels and transferred to polyvinylidene difluoride (PVDF) membranes (Millipore, MA, USA). The membranes were then blocked for 2 h with 5% (w/v) skim milk in Tris-buffered saline containing Tween-20 (TBST) at room temperature before they were incubated overnight at 4 °C with mouse anti-β-actin (1:500, Boster Biological Technology, Ltd., Wuhan, China), rabbit anti-AMPK (1:1000, Affinity, Jiangsu, China), rabbit anti-p-AMPK (1:1000, Affinity, Jiangsu, China), rabbit anti-TLR-4 (1:1000, Affinity, Jiangsu, China), rabbit anti-p65 (1:1000, Abcam, Cambridge, UK), rabbit anti-p-p65 (1:1000, Abcam, Cambridge, UK), and rabbit anti-Nrf2 (1:2000, Proteintech Group, Inc., Wuhan, China) antibodies. The next day, the membranes were incubated with secondary sheep anti-mouse and sheep anti-rabbit antibodies (1:10000, Boster Biological Technology, Ltd., Wuhan, China) for 2 h at room temperature. Next, the excess secondary antibody was washed off the PVDF membranes with TBST, and films were made after chromogenic exposure. Once the films were dried, the gray-scale values of the bands in the film were quantified via BandScan 5.0 (Glyko Inc., CA, USA).

Relative expression of colonic neurons and enteric glial cells (EGCs)

Samples of colon tissue located 6–8 cm away from the anus were cut off quickly and placed in a corresponding marked tissue embedding folder. After the tissue was dehydrated, made transparent, waxed, sliced, baked, dewaxed and antigen repaired, it was blocked with diluted normal goat serum for 30 min before being immersed in diluted anti-S100β (Proteintech Group, Inc., Wuhan, China) in a wet box at 4 °C for 15 h. The sections were subsequently washed with phosphate-buffered saline containing tween (PBST) and dried with absorbent paper. Then, diluted fluorescein isothiocyanate

(FITC)-labeled sheep anti-mouse IgG (Boster Biological Technology, Ltd., Wuhan, China) was added to the sections and incubated for 1 h at 25 °C in a wet box. After the sections were rinsed with PBST again, diluted anti-HuDC (Abcam, Cambridge, UK) was added, and the mixture was incubated for 15 h at 4 °C in a wet box. The samples were subsequently washed with PBST and dried with absorbent paper before the addition of diluted red fluorescent (CY3)-labeled sheep anti-rabbit IgG (Boster Biological Technology, Ltd., Wuhan, China) for 1 h at 25 °C in a wet box. Finally, the sections were washed with PBST before incubation in 4',6-diamidino-2-phenylindole (DAPI) solution for 5 min. After washing again with PBST and sealing with a blocking solution containing an anti-fluorescence quencher, images of the sections were collected via a fluorescence microscope, and IPP 6.0 (Media Cybernetics, MD, USA) was used to analyze the optical density of the regions within the collected photos.

16 S rRNA gene sequencing of gut microbial communities

A QIAamp DNA Mini Kit (Qiagen, Hilden, Germany) was used to isolate fecal DNA. DNA samples were sent to Oebiotech (Shanghai, China) for detection of gene sequences. PCR amplification and Illumina sequencing of the PCR amplicons (Illumina MiSeq platform) were performed via the 250-bp paired-ended strategy to generate raw data. Trimmomatic (Illumina, CA, USA) was used to remove sequences less than 50 bp in length from the raw data, and then Flash was used to splice the sequences. The libraries were subsequently split in QIIME (Illumina, CA, USA) to obtain clean tags. All reads were sorted into different samples according to their barcodes. On the basis of 97% similarity, Vsearch was used to classify valid tags into different operational taxonomic units (OTUs). Principal component analysis (PCA) based on the Uni-Frac distance was performed with QIIME. Linear discriminant analysis (LDA) with effect size measurements (LEfSe) was used to identify indicator bacterial groups specific to these groups.

Statistical analyses

The data are presented as the means \pm standard deviations. One-way analysis of variance (ANOVA) was performed when the data conformed to a normal distribution. When Levene's test of equality of error variance indicated homogeneity of variance, the least significant difference (LSD) method was applied for multiple comparisons, whereas if Levene's test indicated heterogeneity of variance, Dunnett's T3 test for multiple comparisons was performed. If the data did not conform to a normal distribution, they were analyzed by the Kruskal–Wallis test, followed by the Wilcoxon comparison test for pairwise comparisons. A P value < 0.05 was considered to indicate statistical significance. Statistical analysis was performed via SPSS 26 (IBM Corp., Armonk, NY).

Results

The combination of Bifidobacterium and Rosuvastatin increased energy intake but had no significant effect on blood lipids or body weight in MAFLD rats

The vital signs of all the rats in each group were stable during feeding. Body weight began to differ between the rats in Group N and those in the HFD-fed groups (Groups M, P, S, and P-S) at week 6, with the largest differences observed at week 8 (Fig. 1a). After the intervention for 4 weeks, there was no significant difference in body weight among the HFD-fed groups, and there was no difference in body weight between the Group N and the HFD-fed groups (Table 2). The energy intake of the rats in each group changed little in the first 8 weeks but decreased in the 9th week after intervention (Fig. 1b). Over the 12 weeks of the experiment, the energy intake of the rats in Group N was lower than that of the rats in the HFD-fed groups (Fig. 1b). In particular, in the first 8 weeks, the energy intake of the rats in the HFD-fed groups was greater than that of the rats in Group N, whereas no difference was detected among the HFD-fed groups (Table 2). In the final 4 weeks, compared with that in Group N, the energy intake in

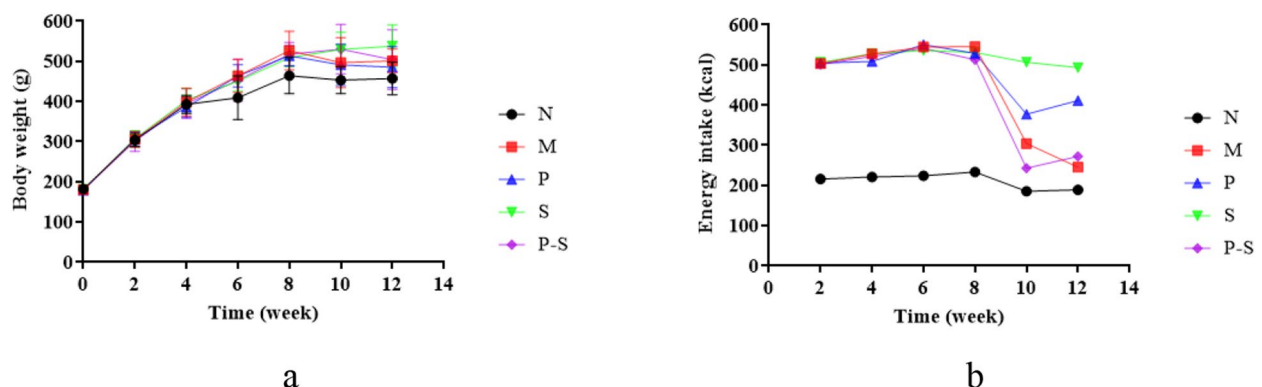


Fig. 1 **a** Changes in the body weights of the rats in each group over time. **b** Changes in food and water intake by the rats in each group over time

Table 2 Body weight and food and water intake of the rats in each group

Group	Body weight on week 8, g	Body weight on week 12, g	Weight gain, g	Energy intake in the first 8 weeks, g	Energy intake in the last 4 weeks, g
N	464.43 ± 45.22	457.00 ± 40.67	277.83 ± 39.17	223.43 ± 10.00	187.04 ± 6.77
M	526.86 ± 47.95 ^{##}	501.33 ± 29.74	322.33 ± 25.56	530.18 ± 19.64 ^{##}	274.70 ± 46.38
P	513.57 ± 25.09 [#]	485.17 ± 50.89	306.83 ± 55.00	523.20 ± 20.82 ^{##}	394.28 ± 23.04 [*]
S	509.14 ± 22.15 [#]	537.67 ± 53.03	354.33 ± 50.44	525.45 ± 20.17 ^{##}	499.98 ± 30.04 ^{**}
P-S	517.57 ± 29.06 ^{##}	504.00 ± 74.19	321.67 ± 74.84	519.25 ± 17.69 ^{##}	257.56 ± 110.51

The data are presented as the means ± standard deviations. 0–7 weeks, n = 8; 8–12 weeks, n = 6, [#]*P* < 0.05 compared with Group N, ^{##}*P* < 0.01 compared with Group N; ^{*}*P* < 0.05 compared with Group M, ^{**}*P* < 0.01 compared with Group M

Table 3 Serum concentrations of TC, TG, HDL-C, and LDL-C in the rats in each group

Group	TC (mmol/L)	TG (mmol/L)	HDL-C (mmol/L)	LDL-C (mmol/L)
N	1.55 ± 0.29	0.6 ± 0.21	0.99 ± 0.25	0.36 ± 0.18
M	1.51 ± 0.47	0.58 ± 0.43	0.96 ± 0.26	0.34 ± 0.06
P	1.50 ± 0.28	0.44 ± 0.18	1.0 ± 0.24	0.33 ± 0.06
S	1.53 ± 0.38	0.55 ± 0.14	0.97 ± 0.21	0.34 ± 0.06
P-S	1.17 ± 0.36	0.44 ± 0.12	0.73 ± 0.13	0.31 ± 0.05

The data are presented as the means ± standard deviations

Group M was still greater, whereas compared with that in Group M, the energy intake in Groups P and S was greater (Table 2). The results of the blood lipid level measurements revealed no significant differences between Group N and Group M and no significant differences among the HFD-fed groups (Table 3).

The combination of *Bifidobacterium* and Rosuvastatin decreased the liver-related indices in MAFLD rats

The liver index and IR index of Group M were greater than those of Group N, and compared with those of Group M, the liver index was lower in Groups P and P-S, and the IR index was lower in Groups P-S (Fig. 2a and b). The AST and ALT levels in Group M tended to be greater than those in Group N, but the difference was not statistically significant (Fig. 2c and d). However, the AST and ALT levels of Group M were greater than those of Groups P-S (Fig. 2c and d).

The combination of *Bifidobacterium* and Rosuvastatin significantly improved liver pathology and reduced MAS in MAFLD rats

Representative images of HE-stained liver tissue from each group after intervention for 4 weeks are shown in Fig. 3a. The hepatic lobules appeared normal for Group

N, with no evidence of hepatic steatosis or inflammatory cell infiltration. The hepatic lobules of Group M were unclear, as the liver cells were enlarged, with the nucleus on one side and lipid droplets in the cytoplasm. In addition, some of the sink areas had inflammatory foci. Compared with Group M, Groups P, S, and P-S improved hepatocyte adipose degeneration and intralobular inflammation. Compared with those of Group N, the MASs of Group M were greater, and the MASs of Groups P, P-S, and S were lower than those of Group M (Fig. 3b).

The combination of *Bifidobacterium* and Rosuvastatin could regulate the TLR-4/NF-κB and AMPK/Nrf2 pathways and reduce the release of inflammatory cytokines in liver tissue

Compared with those in Group N, the relative expression levels of p-AMPK and Nrf2 in Group M were significantly lower, whereas compared with those in Group M, the relative expression levels of p-AMPK and Nrf2 in Groups P, S, and P-S were significantly greater (Fig. 4a and b). Compared with those in Group N, the relative expression levels of TLR-4 and p-p65 in Group M were significantly greater, whereas compared with those in Group M, the relative expression levels of TLR-4 and p-p65 in Groups P, S, and P-S were significantly lower (Fig. 4c and d). Compared with those in Group N, the expression levels of IL-6, IL-1β and TNF-α in Group M were greater, whereas the expression levels of IL-6, IL-1β and TNF-α in Groups N, P, S, and P-S were lower than those in Group M (Fig. 4e, f and g).

Together, these results demonstrated that HFD feeding could downregulate the Nrf2 and p-AMPK within the AMPK/Nrf2 pathway and upregulate TLR-4 and p-p65 within the TLR-4/NF-κB pathway in MAFLD rats, while also increasing IL-6, IL-1β, and TNF-α. However, administration of *Bifidobacterium*, *Rosuvastatin*, and their combination could inhibit these changes.

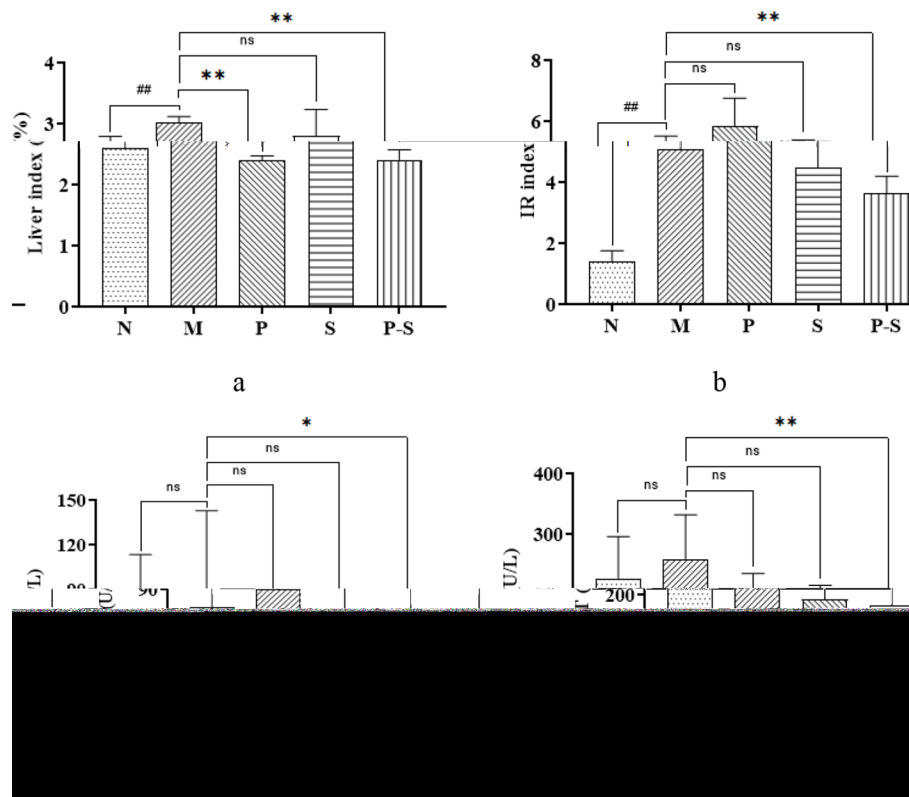


Fig. 2 a, b Liver indices and IR indices of the rats in each group compared by one-way analysis of variance (ANOVA) followed by the least significant difference (LSD) multiple comparison test. ## $P < 0.01$ compared with Group N, ** $P < 0.01$ compared with Group M. c, d ALT and AST levels in each group compared via the Kruskal–Wallis H test. * $P < 0.05$ compared with Group M, ** $P < 0.01$ compared with Group M

The combination of *Bifidobacterium* and Rosuvastatin increased the relative counts of intestinal neurons and EGCs in MAFLD rats

On immunohistochemical staining of intestine sections, intestinal neurons were fluorescently labeled with red, and EGCs were fluorescently labeled with green (Fig. 5a). Compared with those in Group N, the relative counts of intestinal neurons and EGCs were lower in Group M (Fig. 5b and c). Compared with those in Group M, the relative counts of intestinal neurons were greater in Groups S and P-S (Fig. 5b), and the relative counts of EGCs in Groups P, S, and P-S were greater (Fig. 5c).

The combination of *Bifidobacterium* and Rosuvastatin promoted gastrointestinal motility in MAFLD rats

Compared with those in Group N, the intestinal propulsion and gastric emptying rates in Group M were lower, whereas compared with those in Group M, the intestinal propulsion and gastric emptying rates in Groups P and P-S were greater (Fig. 6a and b). Compared with those in Group N, the levels of GT and 5-HT were lower and the

levels of VIP and SST were greater in Group M. Compared with those in Group M, the levels of GT and 5-HT were greater and the levels of VIP and SST were lower in Groups P, S, and P-S (Fig. 6c, d, e and f).

The combination of *Bifidobacterium* and Rosuvastatin could regulate the gut microbiota in MAFLD rats

The numbers of OTUs in each group were as follows (Fig. 7a): 5844 in Group N, 6398 in Group M, 6106 in Group P, 5991 in Group S, and 6236 in Group P-S. The results revealed that the number of OTUs was increased by HFD feeding in rats and that treatment with *Bifidobacterium*, rosuvastatin, or their combination reversed this change in OTUs. A total of 3648 OTUs were detected in all five groups, reflecting a strong core microbiota in the intestinal tract of the rats.

The confidence ellipse for Group M was far from that for Groups N, P, S, and P-S (Fig. 7b). These results revealed that the species composition of Group M was quite different from that of the other groups, whereas the

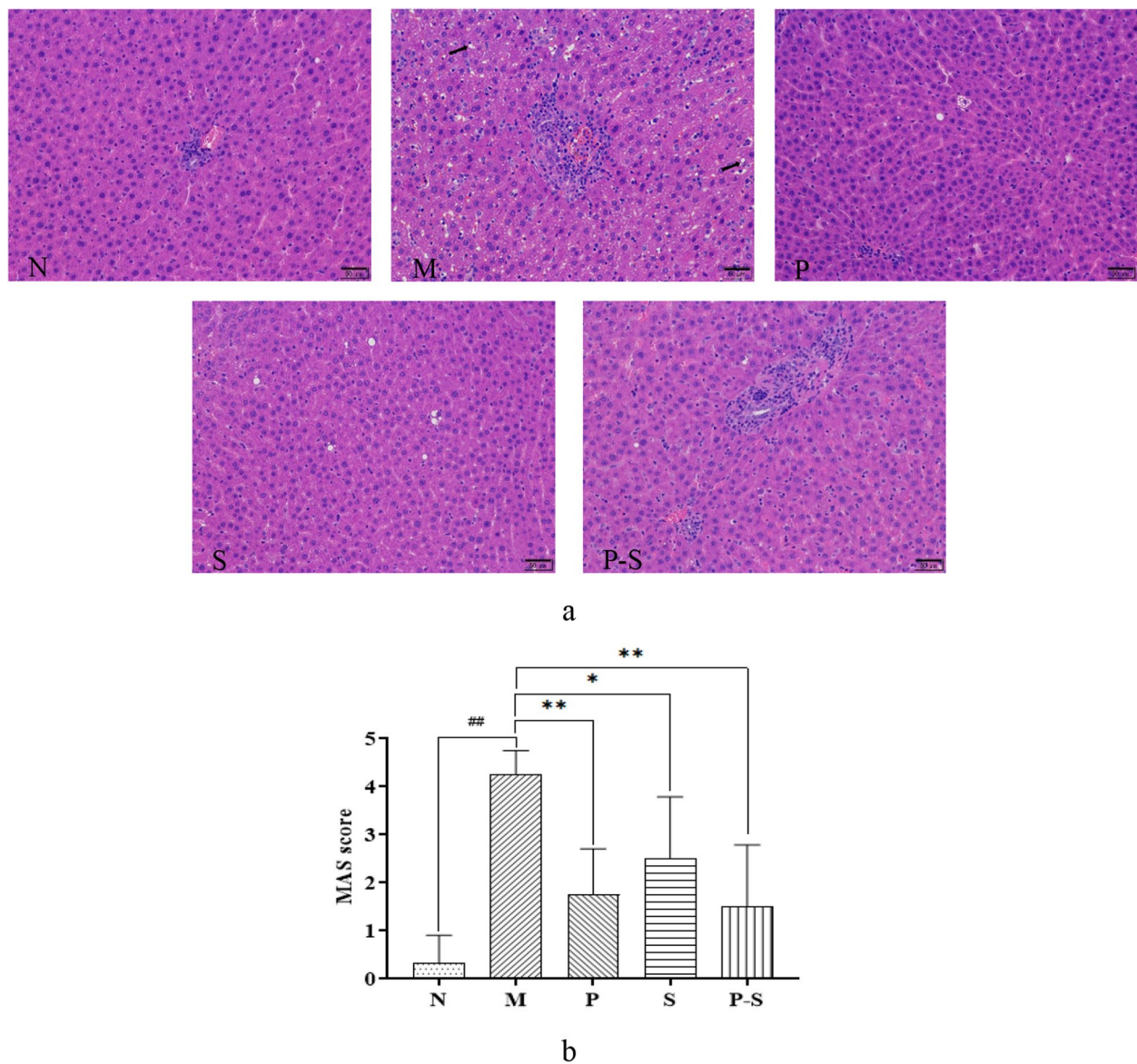


Fig. 3 **a** Representative images of HE-stained liver samples from rats in each group (200x magnification; the black arrows indicate fatty changes). **b** MAS scores for the rats in each group were compared via one-way ANOVA followed by the least significant difference (LSD) multiple comparison test. ## $P < 0.01$ compared with Group N, ** $P < 0.01$ compared with Group M, * $P < 0.05$ compared with Group M

species compositions were similar among the other four groups.

The differences in the gut microbiota species among all five groups were examined via LefSe (Fig. 7c). Group N included three biomarkers, namely, *Escherichia Shigella*,

Ruminococcaceae_UCG-005, and *Ruminiclostridium*, whereas Group M included two biomarkers, namely, *Prevotellaceae_UCG-001* and *Lachnospira*. The remaining three groups did not present genus-level biomarkers. These findings suggest that HFD feeding could alter

(See figure on next page.)

Fig. 4 **a** p-AMPK protein expression in each group compared by one-way ANOVA followed by the Dunnett T3 multiple comparison test. ## $P < 0.01$ compared with Group N, ** $P < 0.01$ compared with Group M. **b–d** Nfr2, TLR-4, and p-p65 protein expression in each group compared by one-way ANOVA followed by the least significant difference (LSD) multiple comparison test. ## $P < 0.01$ compared with Group N, ** $P < 0.01$ compared with Group M. **e–g** TNF- α , IL-1 β , and IL-6 levels in each group were compared by one-way ANOVA followed by the least significant difference (LSD) multiple comparison test. ## $P < 0.01$ compared with Group N, ** $P < 0.01$ compared with Group M

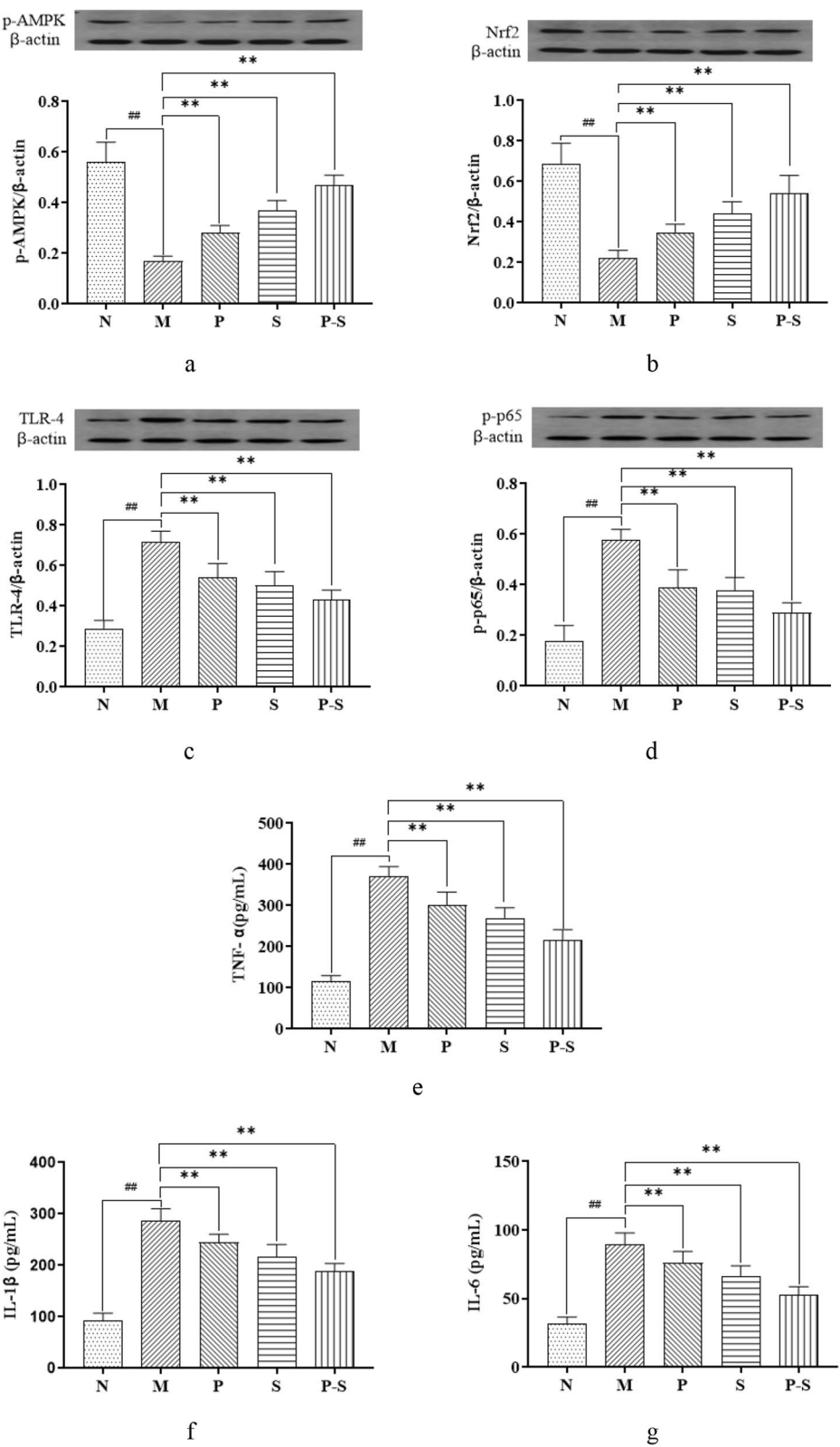


Fig. 4 (See legend on previous page.)

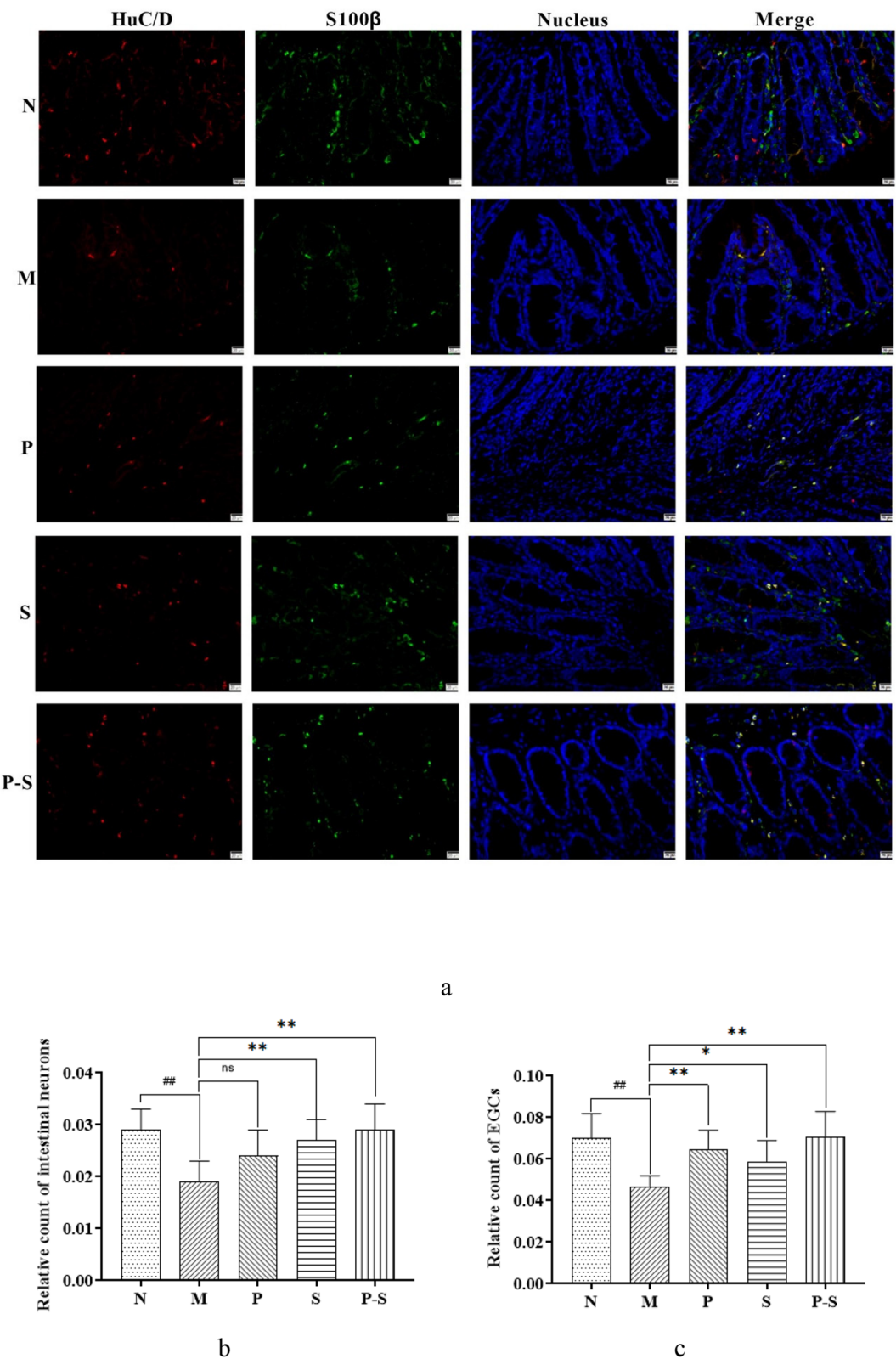


Fig. 5 **a** Merged images of immunohistochemical staining of intestinal neurons (red fluorescence) and EGCs (green fluorescence), with nuclei in blue (200x magnification). **b** Relative counts of intestinal neurons; **c** relative counts of EGCs; both groups were compared by one-way ANOVA followed by the least significant difference (LSD) multiple comparison test. ##*P*<0.01 compared with Group N, ***P*<0.01 compared with Group M, **P*<0.05 compared with Group M

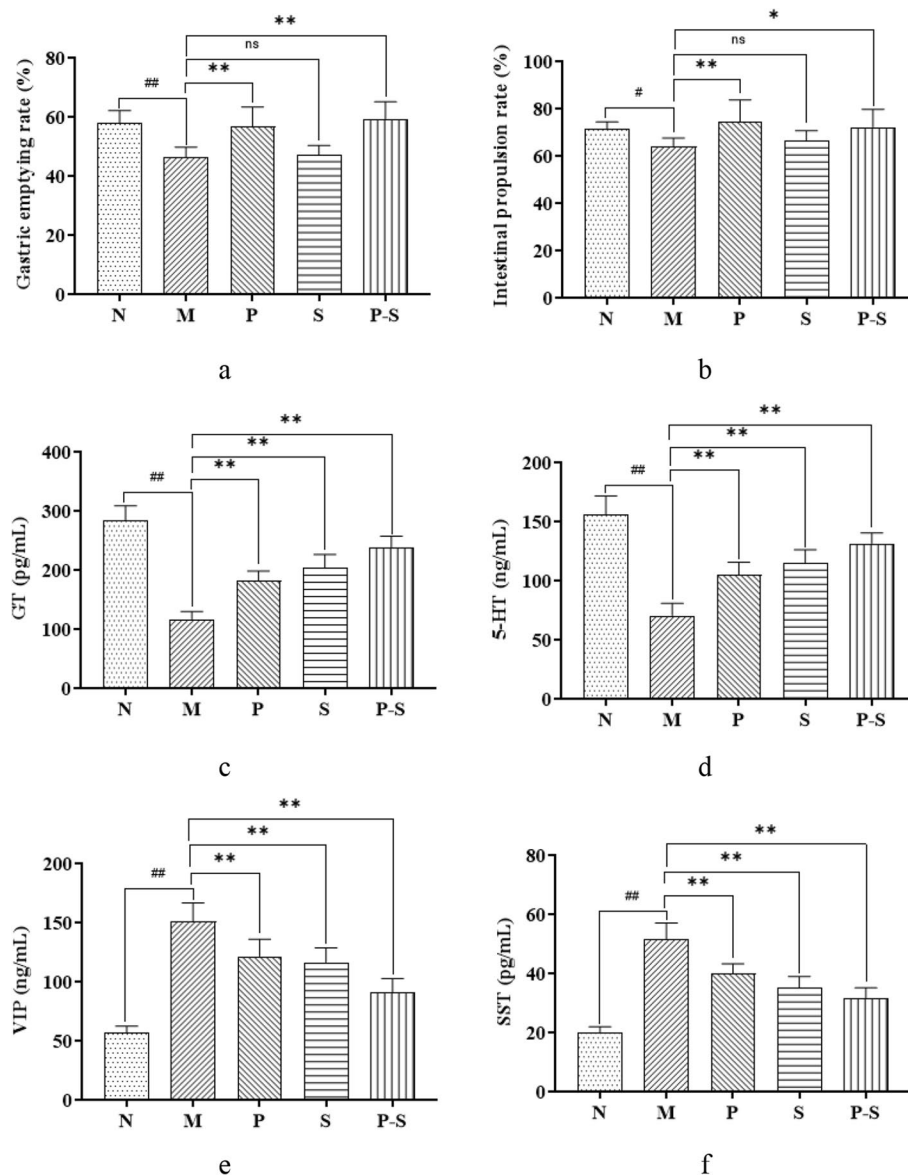
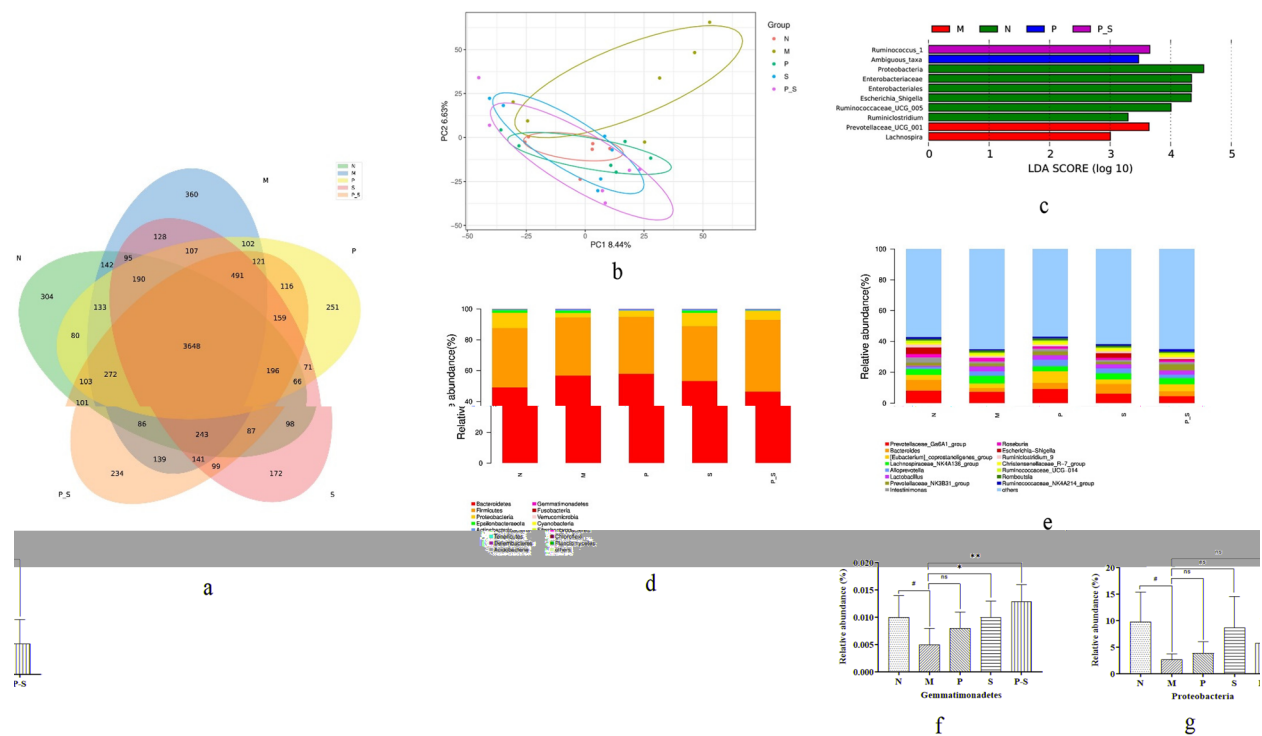


Fig. 6 **a** Gastric emptying; **b** intestinal propulsion; **c** GT level; **d** 5-HT level; **e** VIP level; and **f** SST level, all compared among the groups by one-way ANOVA followed by the LSD multiple comparison test. ## $P < 0.01$ compared with Group N, # $P < 0.05$ compared with Group N, ** $P < 0.01$ compared with Group M, * $P < 0.05$ compared with Group M

the presence of intestinal biomarkers, but treatment with *Bifidobacterium*, rosuvastatin, or their combination could inhibit these alterations without generating new biomarkers.

The gut microbiota of the rats primarily consisted of *Bacteroides*, *Firmicutes*, and *Proteobacteria* at the phylum level, and the sum of the relative abundances (RAs) of *Bacteroides* and *Firmicutes* was close to 90% (Fig. 7d). Compared with those in Group N, the RAs of *Gemmatimonadetes* and *Proteobacteria* in Group M were lower (Fig. 7f and g), whereas compared with those in Group M,

the RAs of *Gemmatimonadetes* in Groups S and P-S were significantly greater (Fig. 7f). The gut microbiota of the rats consisted mainly of *Prevotellaceae_Ga6A1_group*, *Bacteroides*, *[Eubacterium]_coprostanoligenes_group*, and *Lachnospiraceae_NK4A136_group* at the genus level (Fig. 7e). Compared with those in Group N, the RAs of *Sphingomonas*, *Asticcacaulis*, and *Prevotellaceae_UCG-001* were greater, and the RAs of *Escherichia-Shigella* and *Fusobacterium* were lower in Group M (Table 4). Compared with those in Group M, there was an increase in the RA of *Ruminococcaceae_UCG-013*; a decrease in the RA of *Turicibacter*

**Table 4** RAs of the gut microbiota at the genus level in each group

Genus	N	M	P	S	P-S
<i>Sphingomonas</i>	0.005 ± 0.003	0.016 ± 0.009 [#]	0.021 ± 0.007	0.023 ± 0.007	0.027 ± 0.006*
<i>Streptomyces</i>	0.019 ± 0.005	0.018 ± 0.006	0.016 ± 0.006	0.009 ± 0.004**	0.012 ± 0.003*
<i>Ruminococcaceae</i> _UCG-013	0.129 ± 0.080	0.129 ± 0.042	0.215 ± 0.097*	0.085 ± 0.025	0.124 ± 0.060
<i>Odoribacter</i>	0.005 ± 0.005	0.003 ± 0.001	0.006 ± 0.004	0.017 ± 0.004	0.033 ± 0.007**
<i>Escherichia-Shigella</i>	4.084 ± 6.628	0.053 ± 0.046 ^{##}	0.061 ± 0.028	3.156 ± 6.369	0.729 ± 1.533
<i>Fusobacterium</i>	0.004 ± 0.001	0.000 ± 0.001 [#]	0.002 ± 0.002	0.006 ± 0.003**	0.003 ± 0.002
<i>Turicibacter</i>	0.080 ± 0.034	0.142 ± 0.114	0.024 ± 0.018*	0.042 ± 0.066	0.021 ± 0.022*
<i>Asticcacaulis</i>	0.000 ± 0.000	0.004 ± 0.003 [#]	0.004 ± 0.002	0.002 ± 0.002	0.002 ± 0.002
<i>Lachnospiraceae</i> _UCG-001	0.152 ± 0.143	0.135 ± 0.062	0.051 ± 0.021	0.022 ± 0.034*	0.065 ± 0.048
<i>Akkermansia</i>	0.001 ± 0.001	0.000 ± 0.000	0.000 ± 0.000	0.002 ± 0.004	0.014 ± 0.022*
<i>Lachnospira</i>	0.025 ± 0.038	0.195 ± 0.152	0.022 ± 0.018	0.027 ± 0.063*	0.099 ± 0.191
<i>Prevotellaceae</i> _UCG-001	0.286 ± 0.432	1.040 ± 0.266 [#]	0.333 ± 0.432	0.240 ± 0.163	0.881 ± 1.339

The data are presented as the means ± standard deviations. # $P < 0.05$ compared with Group N, ## $P < 0.01$ compared with Group N; * $P < 0.05$ compared with Group M, ** $P < 0.01$ compared with Group M

in Group P; an increase in the RA of *Fusobacterium*; a decrease in the RAs of *Streptomyces*, *Lachnospiraceae*_UCG-001 and *Lachnospira* in Group S; an increase in the

RAs of *Sphingomonas*, *Odoribacter*, and *Akkermansia*; and a decrease in the RAs of *Turicibacter* and *Streptomyces* in Groups P-S (Table 4).

Relationships between the gut microbiota and liver- and gastrointestinal-related indices

Spearman correlation analysis was performed to assess the relationships between the RAs of the 12 genera listed above and the related indices of the gastrointestinal tract and liver. The results revealed that five genera were related to liver function, gastrointestinal hormone levels, inflammatory cytokine production, and the expression levels of pathway-related proteins. Specifically, the RA of *Sphingomonas* was negatively correlated with the ALT and AST levels (both $P < 0.05$), as was the RA of *Odoribacter* (both $P < 0.01$), whereas the RA of *Turicibacter* was positively correlated with the ALT and AST levels (both $P < 0.05$). The RA of *Escherichia-Shigella* was positively correlated with the levels of GT, 5-HT, p-AMPK, and Nrf2 (all $P < 0.05$) and negatively correlated with the levels of VIP, SST, TLR-4, p-p65, TNF- α , IL-1 β , and IL-6 (all $P < 0.05$). The RA of

Asticcacaulis was positively correlated with the levels of VIP, SST, TLR-4, p-p65, TNF- α , IL-1 β , and IL-6 (all $P < 0.05$) and negatively correlated with the levels of GT, 5-HT, p-AMPK, and Nrf2 (all $P < 0.05$). Overall, these results support the idea that activation of the TLR4/NF- κ B signaling pathway can lead to increased production of inflammatory cytokines, which leads to an inflammatory reaction in the liver (Fig. 8).

Discussion

In the present study, HFD feeding significantly increased the body weight, liver index, and IR index of the rats and resulted in successful generation of a MAFLD model. Treatment with *Bifidobacterium* decreased the liver indices of MAFLD model rats, but the application of *Bifidobacterium* combined with rosuvastatin decreased the liver indices, IR indices, ALT concentrations, and AST concentrations in MAFLD model rats.

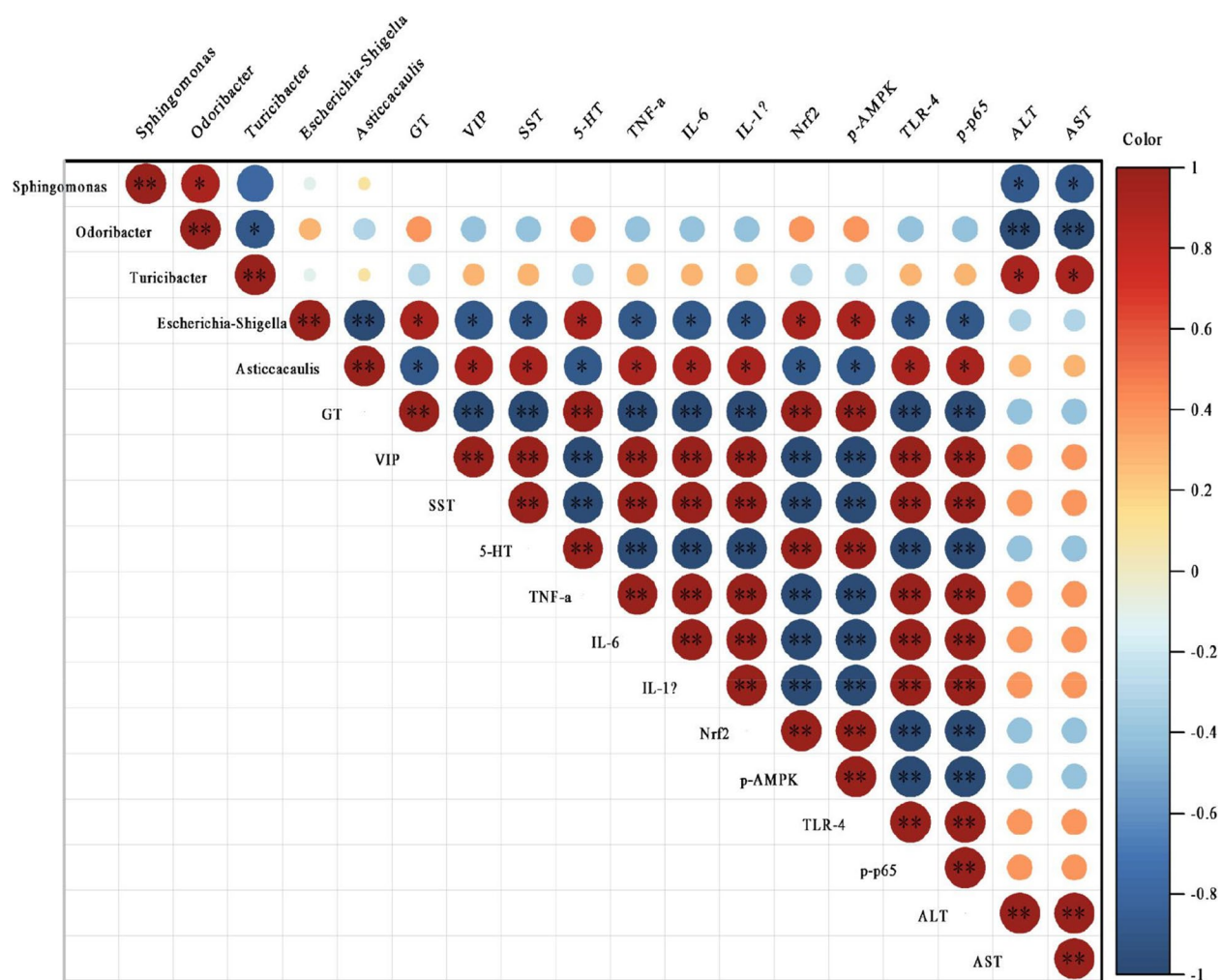


Fig. 8 Correlations between RAs of components of the gut microbiota and liver- and gastrointestinal-related indices. * $P < 0.05$, ** $P < 0.01$. Correlation coefficients > 0 indicate a positive correlation, whereas those < 0 reflect a negative correlation

Bifidobacterium, *rosuvastatin*, and their combination had no effect on the body weight of MAFLD rats, which is consistent with findings in the previous literature [23] showing that *rosuvastatin* has no effect on the body weight of HFD-fed rats. In previous studies, some types of *Bifidobacterium* were able to reduce body weight [24, 25], but in the present study, *Bifidobacterium* had no effect on body weight in rats. This difference may be because the type of *Bifidobacterium* used in this study was different from that used in other studies or because the dose of *Bifidobacterium* administered was small and could not achieve weight loss in HFD-fed animals [26]. Overall, the effect of *Bifidobacterium* on the body weight of HFD-fed rats requires further investigation. Surprisingly, treatment with *Bifidobacterium* or *rosuvastatin* increased the energy intake of the rats, but treatment with their combination did not. According to the literature [18, 24], *Bifidobacterium* and statins have no effect on energy intake. In this study, *Bifidobacterium* increased energy intake, which may be related to its ability to protect appetite [27], whereas the ability of *rosuvastatin* to increase energy intake may be related to *rosuvastatin*-induced diabetes [28]. These results provide new evidence that the combination of *Bifidobacterium* and *rosuvastatin* is relatively effective.

In this study, a HFD led to downregulation of the expression of p-AMPK and Nrf2 in the AMPK/Nrf2 pathway and upregulation of the expression of TLR-4 and p-p65 in the TLR-4/NF- κ B pathway in MAFLD rats. In the MAFLD rat model generated by HFD feeding, the levels of IL-6, IL-1 β , and TNF- α were increased, which promoted pathological changes in the livers of the rats. Treatment with *Bifidobacterium*, *rosuvastatin*, or their combination inhibited these changes and improved liver pathology. The TLR4/NF- κ B pathway is the key pathway that regulates inflammatory mediators. TLR4 is a pattern recognition receptor that can recognize lipopolysaccharides. Once TLR4 is activated by lipopolysaccharide, inhibitors of NF- κ B- α can be phosphorylated, which leads to the phosphorylation of NF- κ B and enables NF- κ B to enter the nucleus, resulting in the release of inflammatory mediators, such as IL-6, IL-1 β , and TNF- α , among others [29]. AMPK acts as the ideal cellular energy charge sensor. After AMPK activation, fatty acid oxidation can be regulated via the phosphorylation of a variety of downstream substrates to maintain the level of ATP [30]. At the gene level, the expression of antioxidants and detoxification enzymes can be regulated by Nrf2. Once cells are subjected to oxidative stress, Nrf2 is released from Keap1 and transferred to the nucleus. This triggers the cellular antioxidant defense response by stimulating the expression of an antioxidant stress gene (HO-1 gene) [31, 32].

In this study, HFD-fed rats presented decreased relative counts of intestinal neurons and EGCs, decreased secretion of GT and 5-HT, increased secretion of VIP and SST, and a reduction in gastrointestinal emptying. Treatment with *Bifidobacterium*, *rosuvastatin*, or their combination increased the secretion of GT and 5-HT and decreased the secretion of VIP and SST, but treatment with *rosuvastatin* did not promote gastrointestinal emptying, and treatment with *Bifidobacterium* did not increase the relative counts of intestinal neurons in MAFLD rats. Previously, neuron enrichment was believed to independently regulate the movement, secretion, and absorption of the gastrointestinal tract, but increasing evidence has suggested that EGCs can not only nourish and support gastrointestinal neurons but also directly and indirectly participate in the regulation of gastrointestinal motility [33]. In this study, HFD consumption led to gastrointestinal dysfunction in rats due to the loss of neurons and EGCs in the colon, which is consistent with previously reported findings [34]. GT and 5-HT can stimulate gastrointestinal smooth muscle to contract and promote gastrointestinal emptying [35, 36]. Conversely, SST and VIP can relax gastrointestinal smooth muscle and slow gastrointestinal emptying [37, 38]. In the present study, treatment with *rosuvastatin* decreased the SST and VIP levels and increased the GT and 5-HT levels but did not promote gastrointestinal emptying, which may be related to the adverse effects of statins. A previous study [39] showed that statins can cause chronic and persistent intestinal motility disorders, change the level of nitric oxide, and affect intestinal peristalsis. Therefore, treatment with the combination of *Bifidobacterium* and *rosuvastatin* had the greatest improvement effect on intestinal neurons, EGCs and gastrointestinal emptying in MAFLD rats.

Many studies have shown that the abundance of *Fusobacterium* is increased in patients with colon cancer and that its metabolism in the intestinal tract results in the production of large amounts of butyrate and hydrogen sulfide. Butyrate, with its anti-inflammatory effect, is the energy source of colon cells, and the highly toxic end product hydrogen sulfide can inhibit the effective utilization of butyrate by colon cells [40]. In the present study, HFD consumption reduced the abundance of *Fusobacterium*, and treatment with *rosuvastatin* inhibited this change. However, unfortunately, metabolites such as butyrate were not measured in the present study; thus, the advantages and disadvantages of *Fusobacterium* need to be further studied. *Ruminococcaceae_UCG-013* is a butyrate-producing bacteria, and butyrate has beneficial effects on the body [41]. Studies have shown that some bacteria in *Turicibacter* have negative physiological effects on the host [42,

43]. Correlation analysis revealed a positive correlation between the RA of *Turicibacter* and liver function, suggesting that treatment with *Bifidobacterium* and *Bifidobacterium* combined with *rosuvastatin* may improve liver function by reducing the RA of *Turicibacter*.

Streptomyces are distributed mainly in soil, and their most important use is in the production of antibiotics [44]. One study [45] showed that the addition of *Streptomyces aureus* can increase the weight of animals, but its effect on the gastrointestinal tract remains unknown. In the present study, treatment with *rosuvastatin* and *Bifidobacterium* combined with *rosuvastatin* reduced the RA of *Streptomyces* in the intestines, but this change was not accompanied by weight loss. Therefore, further research is needed to confirm the link between the RA of *Streptomyces* and body weight. Another study [46] showed that the decrease in liver function and blood lipid levels in rats fed a HFD is related to the decrease in the RA of *Lachnospiraceae_UCG-001* in these rats. In the present study, treatment with *rosuvastatin* reduced *Lachnospiraceae_UCG-001* in HFD-fed rats, indicating that *rosuvastatin* may regulate liver function by reducing the RA of *Lachnospiraceae_UCG-001*.

Many strains in *Lachnospira* are producers of short-chain fatty acids, which act to maintain the normal function of the bowel [44]. In this study, treatment with *rosuvastatin* led to a reduction in *Lachnospira*, and a related study [39] revealed that statins can cause chronic and persistent intestinal motility disorders. Thus, treatment with *rosuvastatin* may lead to gastrointestinal motility disturbance by reducing the RA of *Lachnospira*. Research has shown that *Odoribacter* can produce short-chain fatty acids, and a decrease in the RA of *Odoribacter* is related to many microbiota-related diseases, such as MAFLD, cystic fibrosis, and inflammatory bowel disease [47]. Research has also revealed that treatment with *Odoribacter* can inhibit colon cancer [48]. Correlation analysis revealed a negative correlation between the RA of *Odoribacter* and liver function, indicating that *Bifidobacterium* combined with *rosuvastatin* could improve liver function by increasing the RA of *Odoribacter*. *Akkermansia* is a key participant in metabolism and gastrointestinal diseases and a candidate for probiotics [49]. The combined use of *Bifidobacterium* and *rosuvastatin* was found to increase RA and produce beneficial effects on the body.

Study strengths and limitations

In this study, we observed a comprehensive set of indicators, which once again confirmed the effectiveness of *Bifidobacterium* and *rosuvastatin* on MAFLD. Additionally, we found that the combined use of *Bifidobacterium* and *rosuvastatin* was superior to the individual use, providing

new insights into the treatment of MAFLD. However, we also recognize that there are some limitations to our study. Firstly, our sample size is small/limited, which may restrict the generalizability of our results. Secondly, the failure to observe some indicators means we were unable to emphasize the specific mechanisms of gut–liver axis in this study. Nevertheless, we believe that these limitations can be overcome by future research, such as by measuring bile acid, choline and short-chain fatty acid levels in the future study. In summary, our study provides new directions for the treatment of MAFLD. Despite some limitations, we believe that these findings offer valuable references for future research and practice.

Conclusions

All three treatments improved liver pathology and regulated gastrointestinal hormones, but treatment with *Bifidobacterium* also reduced the liver index, increased beneficial bacteria and the relative counts of EGCs, and promoted gastrointestinal motility. Treatment with the combination of *Bifidobacterium* and *rosuvastatin* also reduced the liver index and IR index, increased beneficial bacteria and the relative counts of intestinal neurons and EGCs, decreased ALT and AST, and promoted gastrointestinal motility.

Abbreviations

MAFLD	Metabolic associated fatty liver disease
HFD	High fat diet
FBG	Fasting blood glucose
INS	Insulin
ELISA	Enzyme-linked immunosorbent assay
EGC	Enteric glial cell
HE	Hematoxylin & eosin
IR	Insulin resistance
ALT	Alanine aminotransferase
AST	Aspartate aminotransferase
AMPK	Activated protein kinase
Nrf2	Nuclear factor-erythroid 2-related factor 2
TLR-4	Toll-like receptor 4
NF-κB	Nuclear factor kappa-B
TNF-α	Tumor necrosis factor-alpha
IL-1β	Interleukin-1beta
IL-6	Interleukin-6
MAS	MAFLD activity score
GT	Gastrin
5-HT	5-Hydroxytryptamine
VIP	Vasoactive intestinal peptide
SST	Somatostatin
MASH	Metabolic-associated steatohepatitis
HCC	Hepatocellular carcinoma
ENS	Enteric nervous system
CFU	Colony-forming unit
IACUC	Institutional Animal Care and Use Committee
TG	Triglycerides
TC	Total cholesterol
HDL	High-density lipoprotein
LDL	Low-density lipoprotein
PMSF	Phenylmethanesulfonyl fluoride
PVDF	Polyvinylidene difluoride
TBST	Tris-buffered saline containing Tween-20
PBST	Phosphate-buffered saline containing Tween-20

FITC	Fluorescein isothiocyanate
DAPI	4',6-Diamidino-2-phenylindole
OTU	Operational taxonomic unit
RDP	Ribosomal Database Project
PCA	Principal component analysis
LDA	Linear discriminant analysis
LEfSe	LDA effect size
ANOVA	Analysis of variance
LSD	Least significant difference
RA	Relative abundance

Acknowledgements

We thank Medjaden Inc. for its assistance in the preparation of this manuscript.

Authors' contributions

All authors contributed to the study conception and design. Material preparation, data collection and analysis were performed by Xue Ran and Ying-jie Wang. Chi-bing Dai and Shi-gang Li participated in the design and guidance of the experiment, assisted in the completion of the experiment and help Xue Ran and Ying-jie Wang with data analysis and manuscript revision. Ran is mainly responsible for the experiment and data processing of the intestine, and Wang is mainly responsible for the experiment and data processing of the liver. They studied different subjects in this experiment. The first draft of the manuscript was written by Xue Ran and Ying-jie Wang, all authors commented on previous versions of the manuscript. All authors read and approved the final manuscript.

Funding

This study was supported in part by grants from the Science Research Project of the Hubei Provincial Health Commission. (WJ2021F060)

Data availability

No datasets were generated or analysed during the current study.

Declarations

Ethics approval and consent to participate

This study was performed in accordance with the principles of the Declaration of Helsinki. Approval was granted by the Ethics Committee of China Three Gorges University (No: 2021ky90).

Consent for publication

Not applicable.

Competing interests

The authors declare no competing interests.

Author details

¹Division of Gastroenterology, Affiliated RenHe Hospital of Three Gorges University, Yichang 443001, China. ²Division of Blood Transfusion Department, Xiang Yang No. 1 People's Hospital, Xiangyang 441099, China. ³Division of Basic Medical Sciences, Three Gorges University, Yichang 443002, China.

Received: 12 June 2024 Accepted: 28 November 2024

Published online: 18 December 2024

References

- Ipsen DH, Lykkesfeldt J, Tveden-Nyborg P. Molecular mechanisms of hepatic lipid accumulation in non-alcoholic fatty liver disease. *Cell Mol Life Sci*. 2018;75(18):3313–27.
- Eslam M, Sanyal AJ, George J. MAFLD: a consensus-driven proposed nomenclature for metabolic associated fatty liver disease. *Gastroenterology*. 2020;158(7):1999–2014.
- Chalasani N, Younossi Z, Lavine JE, Charlton M, Cusi K, Rinella M, et al. The diagnosis and management of nonalcoholic fatty liver disease: practice guidance from the American Association for the study of Liver diseases. *Hepatology*. 2018;67(1):328–57.
- Le MH, Yeo YH, Li X, Li J, Zou B, Wu Y, et al. 2019 global NAFLD prevalence: a systematic review and meta-analysis. *Clin Gastroenterol Hepatol*. 2022;20(12):2809–17.
- Manne V, Handa P, Kowdley KV. Pathophysiology of nonalcoholic fatty liver disease/nonalcoholic steatohepatitis. *Clin Liver Dis*. 2018;22(1):23–37.
- Powell EE, Wong VW, Rinella M. Non-alcoholic fatty liver disease. *Lancet*. 2021;397(10290):2212–24.
- Lonardo A, Ballestri S, Marchesini G, Angulo P, Loria P. Nonalcoholic fatty liver disease: a precursor of the metabolic syndrome. *Dig Liver Dis*. 2015;47(3):181–90.
- Mantovani A, Byrne CD, Bonora E, Targher G. Nonalcoholic fatty liver disease and risk of Incident type 2 diabetes: a meta-analysis. *Diabetes Care*. 2018;41(2):372–82.
- Byrne CD, Targher G. NAFLD: a multisystem disease. *J Hepatol*. 2015;62(1 Suppl):S47–64.
- Noureddin M, Vipani A, Bresee C, Todo T, Kim IK, Alkhoury N, et al. NASH leading cause of liver transplant in women: updated analysis of indications for liver transplant and ethnic and gender variances. *Am J Gastroenterol*. 2018;113(11):1649–59.
- Pouwels S, Sakran N, Graham Y, Leal A, Pintar T, Yang W, et al. Non-alcoholic fatty liver disease (NAFLD): a review of pathophysiology, clinical management and effects of weight loss. *BMC Endocr Disord*. 2022;22(1):63.
- Ji J, Wu L, Wei J, Wu J, Guo C. The gut microbiome and ferroptosis in MAFLD. *J Clin Transl Hepatol*. 2023;11(1):174–87.
- Clare K, Dillon JF, Brennan PN. Reactive oxygen species and oxidative stress in the pathogenesis of MAFLD. *J Clin Transl Hepatol*. 2022;10(5):939–46.
- Albillos A, de Gottardi A, Rescigno M. The gut-liver axis in liver disease: pathophysiological basis for therapy. *J Hepatol*. 2020;72(3):558–77.
- Gomaa EZ. Human gut microbiota/microbiome in health and diseases: a review. *Antonie Van Leeuwenhoek*. 2020;113(12):2019–40.
- de Faria GF, Oliveira DG, de Oliveira JM, de Castro FL, Cesar DE, Moreira A. Influence of gut microbiota on the development and progression of nonalcoholic steatohepatitis. *Eur J Nutr*. 2018;57(3):861–76.
- Ji Y, Yin Y, Li Z, Zhang W. Gut microbiota-derived components and metabolites in the progression of non-alcoholic fatty liver Disease (NAFLD). *Nutrients*. 2019;11:8.
- An HM, Park SY, Lee DK, Kim JR, Cha MK, Lee SW, et al. Antiobesity and lipid-lowering effects of *Bifidobacterium* spp. in high fat diet-induced obese rats. *Lipids Health Dis*. 2011;10: 116.
- Wang L, Jiao T, Yu Q, Wang J, Wang L, Wang G, et al. *Bifidobacterium bifidum* shows more Diversified ways of relieving non-alcoholic fatty liver compared with *Bifidobacterium adolescentis*. *Biomedicines*. 2021;10(1):84.
- Doumas M, Imprialos K, Dimakopoulou A, Stavropoulos K, Binas A, Athyros VG. The role of statins in the management of nonalcoholic fatty liver disease. *Curr Pharm Des*. 2018;24(38):4587–92.
- Jou J, Choi SS, Diehl AM. Mechanisms of disease progression in nonalcoholic fatty liver disease. *Semin Liver Dis*. 2008;28(4):370–9.
- Ren HX, Tang QC, Yan L, Xia H, Luo HS. Evodiamine inhibits gastrointestinal motility via CCK and CCK1 receptor in water-avoidance stress rat model. *Life Sci*. 2018;209:210–6.
- de Las HN, Valero-Munoz M, Ballesteros S, Gomez-Hernandez A, Martin-Fernandez B, Blanco-Rivero J, et al. Factors involved in rosuvastatin induction of insulin sensitization in rats fed a high fat diet. *Nutr Metab Cardiovasc Dis*. 2013;23(11):1107–14.
- Mazloom K, Siddiqi I, Covasa M. Probiotics: how effective are they in the fight against obesity? *Nutrients*. 2019;11(2):258.
- Do MH, Oh MJ, Lee HB, Kang CH, Yoo G, Park HY. *Bifidobacterium animalis* ssp. *lactis* MG741 reduces Body Weight and ameliorates nonalcoholic fatty liver Disease via improving the gut permeability and amelioration of inflammatory cytokines. *Nutrients*. 2022;14(9):1965.
- Usitupa HM, Rasinkangas P, Lehtinen MJ, Makela SM, Airaksinen K, Anglenius H et al. *Bifidobacterium animalis* subsp. *lactis* 420 for Metabolic Health: review of the Research. *Nutrients*. 2020;12(4):892.
- Yu T, Chen C, Yang Y, Wang M, Yang Y, Feng W, et al. Dissecting the association between gut microbiota, body mass index and specific depressive symptoms: a mediation mendelian randomisation study. *Gen Psychiatr*. 2024;37(4):e101412.

28. Lee YJ, Hong SJ, Kang WC, Hong BK, Lee JY, Lee JB, et al. Rosuvastatin versus atorvastatin treatment in adults with coronary artery disease: secondary analysis of the randomised LODESTAR trial. *BMJ*. 2023;383:e75837.
29. Wang M, Cai XF, Zhang SM, Xia SY, Du WH, Ma YL. Alprostadil alleviates liver injury in septic rats via TLR4/NF-kappaB pathway. *Eur Rev Med Pharmacol Sci*. 2021;25(3):1592–9.
30. Long YC, Zierath JR. AMP-activated protein kinase signaling in metabolic regulation. *J Clin Invest*. 2006;116(7):1776–83.
31. Chen Q, Wang T, Li J, Wang S, Qiu F, Yu H et al. Effects of Natural products on Fructose-Induced nonalcoholic fatty liver Disease (NAFLD). *Nutrients*. 2017;9(2):96.
32. Kensler TW, Wakabayashi N, Biswal S. Cell survival responses to environmental stresses via the Keap1-Nrf2-ARE pathway. *Annu Rev Pharmacol Toxicol*. 2007;47:89–116.
33. Seguela L, Gulbransen BD. Enteric glial biology, intercellular signalling and roles in gastrointestinal disease. *Nat Rev Gastroenterol Hepatol*. 2021;18(8):571–87.
34. Beraldi EJ, Borges SC, de Almeida F, Dos SA, Saad M, Buttow NC. Colonic neuronal loss and delayed motility induced by high-fat diet occur independently of changes in the major groups of microbiota in Swiss mice. *Neurogastroenterol Motil*. 2020;32(2):e13745.
35. Schubert ML, Rehfeld JF. Gastric peptides-gastrin and somatostatin. *Compr Physiol*. 2019;10(1):197–228.
36. Lund ML, Egerod KL, Engelstoft MS, Dmytriyeva O, Theodorsson E, Patel BA, et al. Enterochromaffin 5-HT cells-A major target for GLP-1 and gut microbial metabolites. *Mol Metab*. 2018;11:70–83.
37. McIntosh CH. Gastrointestinal somatostatin: distribution, secretion and physiological significance. *Life Sci*. 1985;37(22):2043–58.
38. Krowicki ZK, Hornby PJ. Contribution of acetylcholine, vasoactive intestinal polypeptide and nitric oxide to CNS-evoked vagal gastric relaxation in the rat. *Neurogastroenterol Motil*. 1996;8(4):307–17.
39. Fernandes R, Shaikh I, Wegstapel H. Possible association between statin use and bowel dysmotility. *BMJ Case Rep*. 2012;2012:bcr1020114918.
40. Brennan CA, Garrett WS. *Fusobacterium nucleatum* - Symbiont, opportunist and oncobacterium. *Nat Rev Microbiol*. 2019;17(3):156–66.
41. Liao R, Xie X, Lv Y, Dai J, Lin Y, Zhu L. Ages of weaning influence the gut microbiota diversity and function in Chongming white goats. *Appl Microbiol Biotechnol*. 2021;105(9):3649–58.
42. Chung Y, Ryu Y, An BC, Yoon YS, Choi O, Kim TY, et al. A synthetic probiotic engineered for colorectal cancer therapy modulates gut microbiota. *Microbiome*. 2021;9(1):122.
43. Pena-Rodriguez M, Vega-Magana N, Garcia-Benavides L, Zepeda-Nuno JS, Gutierrez-Silerio GY, Gonzalez-Hernandez LA, et al. Butyrate administration strengthens the intestinal epithelium and improves intestinal dysbiosis in a cholestasis fibrosis model. *J Appl Microbiol*. 2022;132(1):571–83.
44. Bolourian A, Mojtahedi Z. *Streptomyces*, shared microbiome member of soil and gut, as old friends against colon cancer. *Fems Microbiol Ecol*. 2018;94(8):1–4.
45. Angelakis E. Weight gain by gut microbiota manipulation in productive animals. *Microb Pathog*. 2017;106:162–70.
46. Liu Q, Cai BY, Zhu LX, Xin X, Wang X, An ZM, et al. Liraglutide modulates gut microbiome and attenuates nonalcoholic fatty liver in db/db mice. *Life Sci*. 2020;261: 118457.
47. Hiippala K, Barreto G, Burrello C, Diaz-Basabe A, Suutarinen M, Kainulainen V, et al. Novel *Odoribacter splanchnicus* strain and its outer membrane vesicles exert Immunoregulatory effects in vitro. *Front Microbiol*. 2020;11:575455.
48. Oh BS, Choi WJ, Kim JS, Ryu SW, Yu SY, Lee JS, et al. Cell-free supernatant of *Odoribacter splanchnicus* isolated from human feces exhibits anti-colorectal Cancer activity. *Front Microbiol*. 2021;12:736343.
49. Zhang T, Li Q, Cheng L, Buch H, Zhang F. *Akkermansia muciniphila* is a promising probiotic. *Microb Biotechnol*. 2019;12(6):1109–25.

Publisher's Note

Springer Nature remains neutral with regard to jurisdictional claims in published maps and institutional affiliations.